

Original Article

Effects of shikonin and fisetin on dapsonе metabolism *in vitro* and *in vivo*

Hualu Wu^a, Haoxin Fu^{a,b}, Jun Wu^a, Peiqi Wang^a, Yuxin Shen^a, Lu Shi^{a,*}, Ren-ai Xu^{a,b,*}

^aDepartment of Pharmacy, The First Affiliated Hospital of Wenzhou Medical University, Wenzhou, China

^bZhejiang Key Laboratory of Intelligent Cancer Biomarker Discovery and Translation, First Affiliated Hospital, Wenzhou Medical University, Wenzhou, Zhejiang, China

ARTICLE INFO

Keywords:

Dapsonе
Drug-drug interactions
Fisetin
Inhibition mechanism
Shikonin

ABSTRACT

Dapsonе, a sulfonamide compound commonly used in the treatment of leprosy and herpes, is metabolized by cytochrome P450 to dapsonе hydroxylamine, which in turn causes methemoglobinemia and hemolysis. Consequently, the interaction of dapsonе with other pharmaceutical agents has been the subject of investigation for researchers. In the present study, we conducted a screening of 48 traditional Chinese medicines that may have the potential to exert inhibitory effects in conjunction with dapsonе. We focused on the *in vitro* and *in vivo* drug-drug interactions of dapsonе with shikonin or fisetin. In rat liver microsomes (RLM), the half-maximum inhibitory concentration (IC₅₀) values for shikonin and fisetin were 12.21 μM and 4.97 μM, respectively, and the types of inhibition of dapsonе metabolism were non-competitive in both. In human liver microsomes (HLM), the IC₅₀ values of shikonin and fisetin were 31.39 μM with non-competitive inhibition and 15.00 μM with mixed-type inhibition, respectively. In the Sprague-Dawley (SD) rat pharmacokinetic assay, the plasma exposure of dapsonе significantly increased after the co-administration of shikonin or fisetin. When shikonin and dapsonе were co-administered, the AUC_(0-t) and AUC_(0-∞) of dapsonе exhibited an increase of 0.37 and 0.36 times, respectively, while the CL_{z/F} exhibited a significant 0.27-fold reduction. Moreover, in combination with fisetin, the AUC_(0-t) and AUC_(0-∞) exhibited an increase of 0.30-fold and 0.33-fold, respectively, with a near doubling of the C_{max} and a notable decrease in the CL_{z/F} by 0.23-fold. The metabolite dapsonе hydroxylamine showed no statistically significant differences. It could be concluded that shikonin and fisetin inhibited dapsonе metabolism *in vitro* and *in vivo*. Therefore, when used in clinical association, it is important to monitor the plasma concentration of dapsonе and dapsonе hydroxylamine and make appropriate adjustments to the dosage of dapsonе to minimize the risk of adverse reactions and achieve personalized treatment.

1. Introduction

Dapsonе (4,4'-diaminodiphenylsulfone) is a synthetic derivative of sulfone [1], which has been widely used in recent decades for the treatment of leprosy and other immune disorders [2]. It inhibits the migration of neutrophils from circulation to the site of the lesion, thereby serving as the drug of choice for suppression of the symptoms of herpetic dermatitis [3]. Dapsonе hydroxylamine is an active metabolite of dapsonе, formed primarily through metabolism by CYP3A4 and CYP2E1 [4,5]. It is the primary molecule behind the various adverse reactions associated with dapsonе, including dapsonе hypersensitivity syndrome (DHS) and hemolysis [6,7]. Consequently, it is important to monitor the concentration of dapsonе hydroxylamine after clinical administration of dapsonе.

In recent decades, there has been prominent research on the potential of traditional Chinese medicines in the prevention and treatment of inflammatory diseases and cancer. A number of active ingredients present in traditional Chinese medicines have been demonstrated to possess anti-inflammatory, pro-inflammatory, and anti-neoplastic properties [8]. Shikonin, a naphthoquinone compound extracted from comfrey, has been the subject of extensive study due to its diverse range of biological activities, including anticancer, wound healing,

and anti-inflammatory effects [9,10]. In recent years, the capacity of shikonin to facilitate skin healing has been demonstrated in a number of dermatological conditions, including melanoma, hyperplastic scars, and psoriasis [11]. Fisetin, a naturally occurring flavonoid and an active ingredient of *Cotinus coggygria*, has been demonstrated to possess anticancer and anti-inflammatory properties [12,13]. It has been demonstrated that fisetin can induce autophagosome-lysosome fusion, thereby promoting autophagy and differentiation [14]. Consequently, fisetin has the potential to alleviate psoriasis-like dermatitis and reduce excessive keratinization. Both shikonin and fisetin have been demonstrated to exert inhibitory effects on the CYP3A4 enzyme, and have been shown to possess therapeutic properties for dermatological conditions [15,16]. Therefore, it is possible to combine dapsonе with these agents, making this study of practical significance.

In this study, the most probable drug-drug interactions between dapsonе and 48 distinct traditional Chinese medicines were identified to determine whether they might exert inhibitory effects *in vitro*. Furthermore, the effects of shikonin and fisetin on dapsonе metabolism were validated in Sprague-Dawley (SD) rats, and the underlying inhibitory mechanisms were investigated *in vitro*. In instances where dapsonе is indicated in conjunction with other pharmaceutical agents, it is imperative to meticulously monitor the plasma concentrations

*Corresponding authors:

E-mail addresses: xra@wmu.edu.cn (Ren-ai Xu), shilu199004@163.com (Lu Shi)

Received: 21 September, 2024 Accepted: 20 February, 2025 Epub Ahead of Print: 16 April 2025 Published: 21 May 2025

DOI: 10.25259/AJC_34_2024

of dapsone and dapsone hydroxylamine to reduce the likelihood of unfavorable responses occurring during clinical administration.

2. Materials and Methods

2.1. Chemicals and reagents

Dapsone (Figure 1a), dapsone hydroxylamine (Figure 1b), fisetin (Figure 1c), shikonin (Figure 1d), fluconazole (used as internal standard, IS), and 46 other traditional Chinese medicines were bought from Shanghai Canspec Scientific Instruments Co., Ltd. (Shanghai, China). The human liver microsomes (HLM) was procured from iPhase Pharmaceutical Services Co., Ltd. (Jiangsu, China). The reagents were procured from the following sources: nicotinamide adenine dinucleotide phosphate (NADPH) from Shanghai Aladdin Biochemical Technology Co., Ltd. (Shanghai, China), methanol and acetonitrile in LC grade from Merck (Darmstadt, Germany) and formic acid from Anaqua Chemicals Supply (ACS, USA). The preparation of ultrapure water was conducted utilizing a Milli-Q water purification system, provided by Millipore (Bedford, MA, USA). The remaining chemicals and reagents were also of LC grade.

2.2. Detection conditions

Chromatographic separation was conducted using an Acquity ultra-performance liquid chromatography (UPLC) system (Waters Corp., Milford, MA, USA) with an Acquity BEH C18 column (2.1 mm × 50 mm, 1.7 μm) at 40°C. The mobile phase comprised of 0.1% formic acid (solution A) and acetonitrile (solution B) at a flow rate of 0.4 mL/min. The injection volume and time for each sample were 2.0 μL and 2.0 mins, respectively. The analytes were eluted in a gradient. The elution process was divided into five distinct stages, as outlined below: 0–0.5 min (solution A, 90%), 0.5–1.0 min (solution A, 90%–10%), 1.0–1.4 min (solution A, 10%), 1.4–1.5 min (solution A, 10%–90%), 1.5–2.0 min (solution A, 90%).

Quantification was conducted using a Waters Xevo TQ-S triple quadrupole tandem mass spectrometer. The ion leaps of dapsone, dapsone hydroxylamine, and IS were detected in positive mode using multiple reaction monitoring (MRM). The data pertaining to particular ion pairs and associated with collision energies has been presented in Table 1.

2.3. Rat liver microsomes (RLM) preparation

Six untreated rat livers were rinsed three times with cold phosphate-buffered saline (PBS) and weighed. The tissue was finely chopped and combined with 0.25 mM sucrose-PBS in a 2.5:1 ratio. The resulting

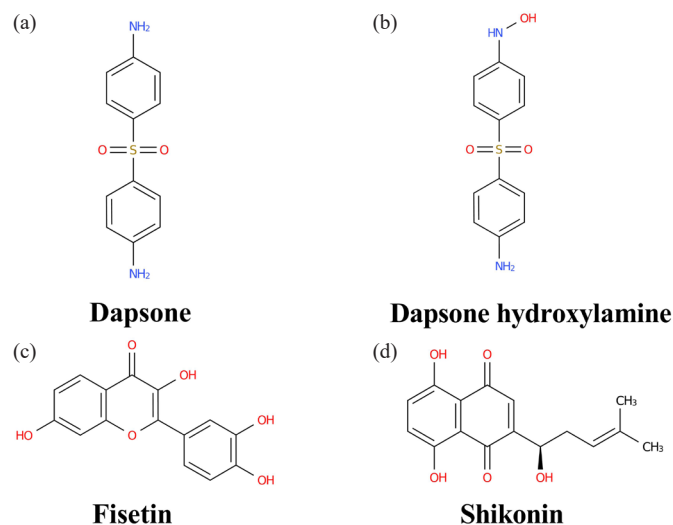


Figure 1. Chemical structural formulas: (a) dapsone, (b) dapsone hydroxylamine, (c) fisetin, and (d) shikonin.

Table 1. Mass spectrum parameters of dapsone, dapsone hydroxylamine and fluconazole.

Compound name	Parent (m/z)	Daughter (m/z)	Cone (V)	Collision (eV)
Dapsone	248.96	107.91	30	15
Dapsone hydroxylamine	264.93	107.91	30	18
Fluconazole	307.14	220.12	6	16

mixture was subsequently homogenized. The resulting homogenate was then ultracentrifuged at 11,000 rpm for 15 mins at 4°C. The resulting precipitate was discarded, and the supernatant was subjected to the same process twice. The resulting supernatant was subjected to ultracentrifugation (75,600 × g, 2 hrs, 4°C). The precipitate obtained was then diluted with 2 to 3 times cold PBS. This diluted solution was then poured back into the same centrifuge tube to facilitate homogenization and stored in portions at –80°C [17]. The protein concentrations were determined utilizing the Bradford Protein Assay Kit (Thermo Scientific).

2.4. Determination of the Michaelis-Menten constant (K_m) for dapsone

The incubation system, with a volume of 190 μL, contained PBS, RLM, or HLM (final concentration: 0.3 mg/mL) and a series of concentration gradients of dapsone (in RLM: 0.1, 1, 2, 5, 10, 20, 50, 100, 200 μM, and in HLM: 15, 75, 150, 300, 450, 600, 750 μM). The incubation system was incubated in a 37°C water bath for a 5-min pre-incubation period. Subsequently, 10 μL of NADPH was added to the incubation system, and the mixture was incubated for 40 mins. Lastly, the samples were stored at –80°C. Once the enzymatic reaction had been completed, 400 μL of acetonitrile and 20 μL of IS working solution were added to the frozen samples. The samples were then vortexed for 2 mins and subjected to centrifugation (13,000 rpm, 10 mins, 4°C) following thawing. A total of 100 μL of the supernatant was subjected to quantitative analysis of the analytes by UPLC-MS/MS to determine the K_m .

2.5. Screening of traditional Chinese medicines for potential interactions with dapsone in RLM

The incubation system, with a volume of 190 μL, contained PBS, RLM (final concentration: 0.3 mg/mL), dapsone (K_m : 32.39 μM), and 48 traditional Chinese medicines (100 μM). The samples were pre-incubated at 37°C for 5 mins prior to the addition of NADPH (1.0 mM). Subsequently, the solution was incubated for 40 mins. Thereafter, the samples were placed in cryogenic storage at –80°C. Then, the samples were processed using the aforementioned steps to ascertain the extent of dapsone metabolism inhibition by the 48 traditional Chinese medicines. Traditional Chinese medicines with relative activity less than 20% were used for screening, and there were 16 such drugs.

A total of 8 out of the 16 selected traditional Chinese medicines were included in the subsequent study. To gain further insight into the inhibitory potencies of these 8 traditional Chinese medicines, the half-maximum inhibitory concentration (IC_{50}) was obtained for comparison. A smaller IC_{50} value indicates greater inhibition of dapsone metabolism. In RLM, the incubation system had a total volume of 190 μL, consisting of PBS, RLM (final concentration: 0.3 mg/mL), dapsone (K_m : 32.39 μM), and a series of concentration gradients of inhibitors (0.01, 0.1, 1, 10, 25, 50, 100 μM). The samples were incubated for 5 mins, followed by the addition of 10 μL of NADPH and an additional 40 mins of incubation. Thereafter, the samples were placed in cryogenic storage at –80°C. The subsequent steps of sample treatment were conducted as previously described to obtain the IC_{50} value of each drug. While in HLM, the IC_{50} values of shikonin and fisetin were determined in a 190 μL incubation system containing PBS, HLM (final concentration: 0.3 mg/mL), dapsone (K_m : 151.00 μM), and shikonin (0.1, 1, 10, 25, 50, 100, 500 μM), or fisetin (0.01, 0.1, 1, 10, 25, 50, 100 μM).

2.6. Inhibitory mechanism of shikonin and fisetin on dapsone *in vitro*

To further investigate the mechanism of inhibition of dapsone by shikonin and fisetin *in vitro*, the 190 μL incubation system contained PBS, RLM, or HLM (final concentration: 0.3 mg/mL), dapsone, and

shikonin or fisetin. The pre-incubation mixture was subjected to an initial incubation period of 5 mins, after which 1.0 mM NADPH was added. The mixture was then incubated for 40 mins, followed by a transfer to a temperature of -80°C . Subsequent samples underwent a post-treatment procedure that mirrored the method outlined in Section 2.4. The concentrations of dapson, shikonin, and fisetin were established in accordance with the K_m and IC_{50} values. In RLM, the concentration ranges of dapson, shikonin, and fisetin were 8.10 to 64.78 μM , 0 to 24.42 μM , and 0 to 4.97 μM , respectively. In HLM, the ranges of concentration for dapson, shikonin, and fisetin were 37.75 to 302.00 μM , 0 to 62.78 μM , and 0 to 30.00 μM , respectively. The treatment steps were identical to those previously described.

2.7. Animal experiment

Fifteen male SD rats (200-220 g) utilized in the experiment were sourced from the Animal Experimental Centre of the First Affiliated Hospital of Wenzhou Medical University (Zhejiang, China). The entire experiment was supervised and approved by the Institutional Animal Care and Use Committee of the First Affiliated Hospital of Wenzhou Medical University (Approval No. WYYY-IACUC-AEC-2023-031). Prior to the pharmacokinetic experiment, the 15 rats were randomly assigned to three groups, with five rats in each group. Group A was designated as the control, and Groups B and C represented the experimental groups. A fasting period of 12 hrs was initiated in the rats prior to commencing the experimental procedure, during which water was permitted freely. Dapson was dissolved in corn oil to create a solution, but both shikonin and fisetin were dissolved in 0.5% sodium carboxyl methyl cellulose (CMC-Na) solution. The drug was administered orally *via* gavage to the rats. The doses of dapson, shikonin, and fisetin were determined based

on previous literature [18-20]. At the outset of the experiment, 20 mg/kg of shikonin and 30 mg/kg of fisetin were administered to Group B and C, respectively. Following a 30-min interval, 10 mg/kg of dapson was administered to all three groups. Blood samples were obtained from the rat tail veins at 0.25, 0.5, 0.75, 1, 1.5, 2, 3, 4, 6, 12, 24 and 36 hrs. The samples were then subjected to centrifugation at 13,000 rpm for 10 mins, following which 100 μL aliquots of the supernatant were obtained. Acetonitrile and the IS working solution were added to the plasma in a ratio of 3:1, followed by vortexing and centrifugation at 13,000 rpm for 10 mins. Subsequently, 100 μL of the supernatants were employed for the quantitative analysis of dapson and dapson hydroxylamine by UPLC-MS/MS.

2.8. Data analysis

The graphs and *in vitro* kinetic parameters generated in this study were plotted and calculated using GraphPad Prism (version 8.3.0). The pharmacokinetic parameters were output by Drug and Statistics (DAS) software (version 2.0). Statistical analysis comparing pharmacokinetic parameters across three groups was performed using SPSS software (version 25.0) through One-way Analysis of Variance (ANOVA) test, and significance was defined as a P-value below 0.05.

3. Results and Discussion

3.1. Optimization of UPLC-MS/MS

As illustrated in Figure 2, the dependable and effective UPLC-MS/MS analytical approach was employed to eliminate the impact of interference peaks and successfully separate dapson, dapson

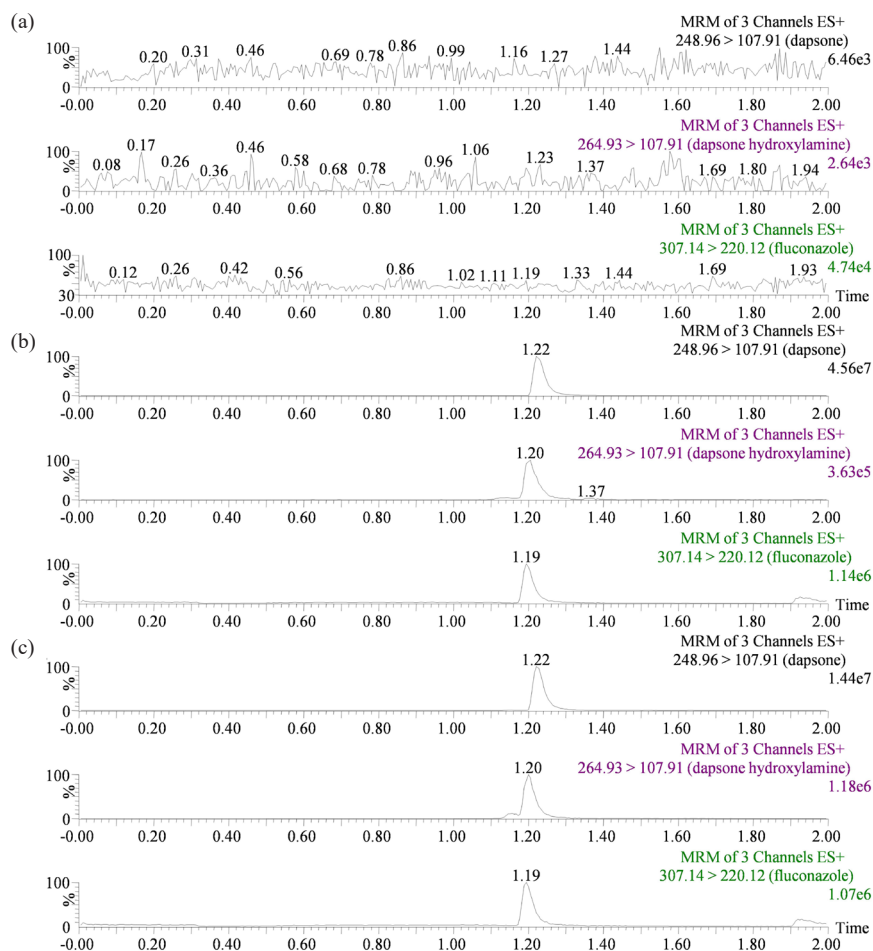


Figure 2. Representative chromatograms: (a) Blank plasma free of IS and analytes; (b) The presence of IS and analytes in blank plasma; (c) sample containing IS and analytes after oral administration of 10 mg/kg dapson from SD rats. SD: Sprague-Dawley.

hydroxylamine, and IS, which exhibited peak times of 1.22, 1.20, and 1.19 min, respectively. Furthermore, the chromatographic conditions were also optimized during the experiment. The separation was conducted on an Acquity BEH C18 column (2.1 mm × 50 mm, 1.7 μm). The results demonstrated that the optimal peak types and responses of the analytes could be achieved when the mobile phase was comprised of a solution of 0.1% formic acid and acetonitrile. By optimizing the mass spectrometry analysis conditions, it was demonstrated that the analytes exhibited high responsiveness and stability in the positive ion mode. The mass spectrometry results of dapsone, dapsone hydroxylamine, and IS demonstrated that the parent ions were most prevalent at m/z values of 248.96, 264.93, and 307.14, respectively.

3.2. Determination of K_m and screening of traditional Chinese medicines

Michaelis-Menten plots were constructed based on the relationship between reaction rate and dapsone concentration, as illustrated in Figure 3. The K_m of dapsone was determined to be 32.39 μM and 151.00 μM in RLM and HLM, respectively. The influence of 48 distinct traditional Chinese medicines on dapsone metabolic rate is demonstrated in Figure 4(a). Of these, 16 traditional Chinese medicines demonstrated the metabolic inhibition of dapsone exceeding 80%, resulting in a metabolic rate of dapsone that was less than 20% (Figure 4b). Subsequent IC_{50} experiments were conducted on 8 of the aforementioned drugs: resveratrol, isorhamnetin, genistein, curcumin, luteolin, kaempferol, shikonin, and fisetin. The IC_{50} values for these drugs in RLM were as follows: 13.79 μM, 14.73 μM, 34.29 μM, 10.93 μM, 7.16 μM, 4.61 μM, 12.21 μM, and 4.97 μM, respectively (Figure 5(a–f) and Figure 6a and b).

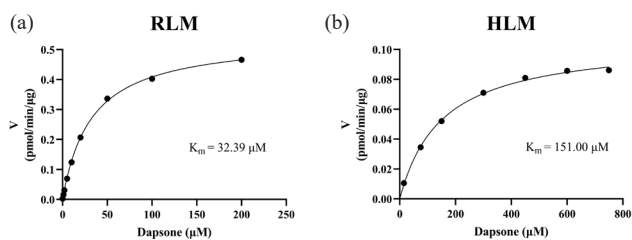


Figure 3. Michaelis-Menten plots of dapsone in (a) RLM and (b) HLM. HLM: Human liver microsomes, RLM: Rat liver microsomes.

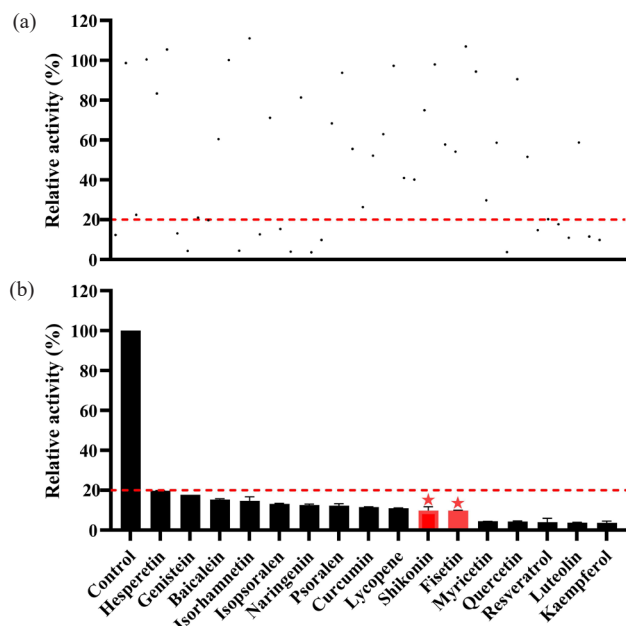


Figure 4. (a) Metabolism rate of dapsone in RLM by 48 traditional Chinese medicines (100 μM); (b) 16 traditional Chinese medicines with metabolism rate less than 20%. RLM: Rat liver microsomes.

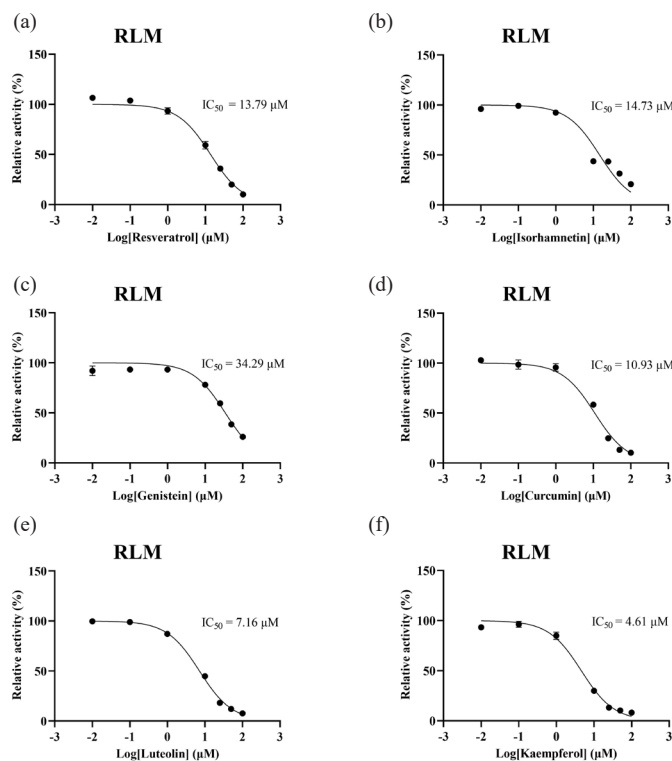


Figure 5. IC_{50} curves of 6 traditional Chinese medicines. (a) Resveratrol, (b) isorhamnetin, (c) genistein, (d) curcumin, (e) luteolin, (f) kaempferol on the metabolic inhibition of dapsone in RLM. HLM: Human liver microsomes, RLM: Rat liver microsomes.

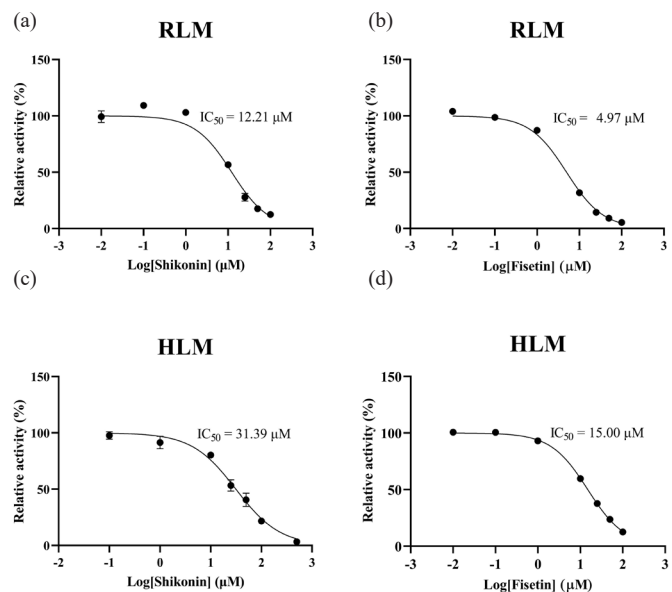


Figure 6. IC_{50} curves of dapsone metabolism in (a and b) RLM and (c and d) HLM by shikonin and fisetin. HLM: Human liver microsomes, RLM: Rat liver microsomes.

3.3. Inhibitory effects of shikonin and fisetin on dapsone in vitro

To gain further insight into the inhibitory potency of shikonin and fisetin, IC_{50} experiments were conducted in HLM. The results demonstrated that the IC_{50} values of shikonin and fisetin in HLM were 31.39 μM and 15.00 μM, respectively (Figure 6c and d). With a 2- to 3-fold difference from the IC_{50} values obtained in RLM, it was clear that shikonin and fisetin had stronger metabolic inhibition of dapsone in RLM. In RLM and HLM, the mechanisms of inhibition on dapsone metabolism by both shikonin and fisetin were further investigated

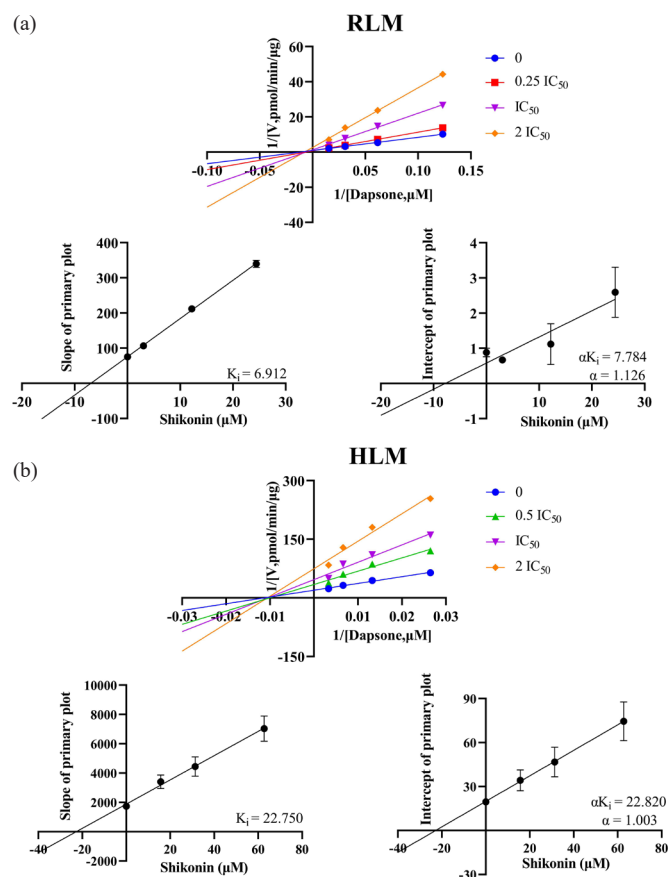


Figure 7. In (a) RLM and (b) HLM, Lineweaver-Burk plots, K_i secondary plots and αK_i secondary plots of inhibition of dapson metabolism by different concentrations of shikonin. HLM: Human liver microsomes, RLM: Rat liver microsomes.

using double reciprocal diagrams of reaction rate versus dapson concentration. K_i , the inhibition constant, was employed to quantify the inhibitory effect on a substrate, with a lower value denoting more potent inhibition. These plots, which are commonly referred to as Lineweaver-Burk plots, were complemented by the addition of K_i secondary plots and αK_i secondary plots. In the **Figures 7** and **8** the Lineweaver-Burk plots demonstrated that in RLM, all linear clusters intersected the negative half of the X-axis (**Figure 7a** and **Figure 8a**), and both shikonin and fisetin appeared to inhibit dapson metabolism in a non-competitive manner. In HLM, when shikonin was the inhibitor, the linear cluster intersected the negative half-axis of the X-axis (**Figure 7b**), and when fisetin was the inhibitor, the linear cluster intersected in the second quadrant (**Figure 8b**), indicating that shikonin and fisetin inhibited dapson metabolism in non-competitive and mixed manners, respectively. The IC_{50} values, type of inhibition, αK_i and α values for dapson inhibition by shikonin and fisetin in RLM and HLM have presented in **Tables 2** and **3**, respectively. Consequently, both shikonin and fisetin had been observed to inhibit the metabolism of dapson in liver microsomes *in vitro*.

3.4. Pharmacokinetics experiment in SD rats

The inhibitory effects of shikonin and fisetin on dapson were verified in SD rats, and the plasma concentration-time curves of dapson and dapson hydroxylamine have been presented in **Figure 9**. The results indicated a significant increase in plasma exposure to dapson in the cohort that received a combination of shikonin and dapson, in comparison to the control group (administered with dapson alone). This elevation was observed to be 0.37-fold for $AUC_{(0-1)}$ and 0.36-fold for $AUC_{(0-\infty)}$. Regarding $CL_{z/F}$, a significant decrease from 0.44 ± 0.06 L/h/kg to 0.32 ± 0.04 L/h/kg ($p < 0.05$) was observed. In comparison

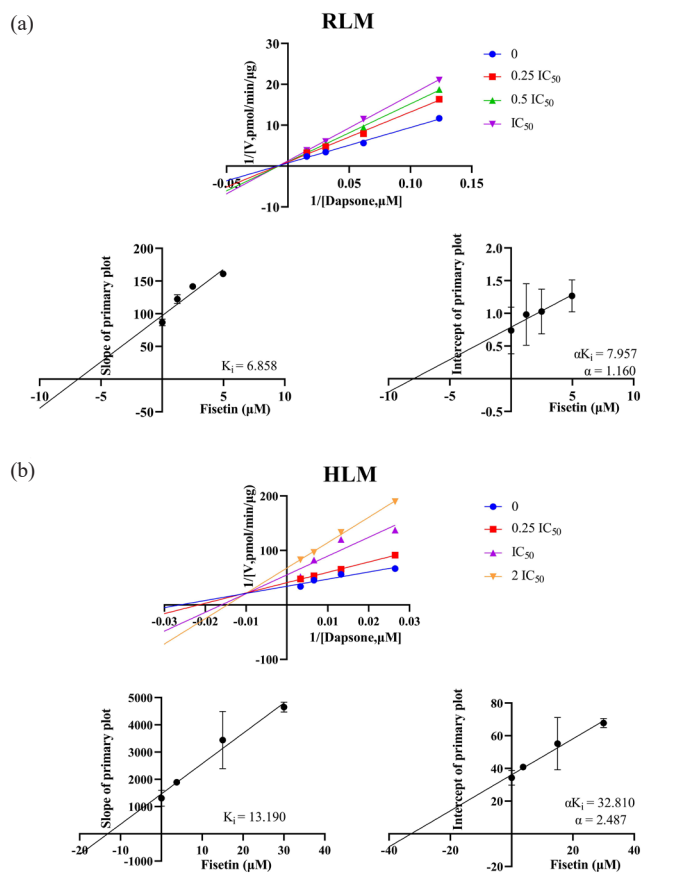


Figure 8. In (a) RLM and (b) HLM, Lineweaver-Burk plots, K_i secondary plots and αK_i secondary plots of inhibition of dapson metabolism by different concentrations of fisetin. HLM: Human liver microsomes, RLM: Rat liver microsomes.

Table 2. IC_{50} values and inhibition of dapson metabolism by shikonin in RLM and HLM.

	IC_{50} Value (μM)	Inhibition type	K_i (μM)	αK_i (μM)	α
RLM	12.21	Non-competitive inhibition	6.912	7.784	1.126
HLM	31.39	Non-competitive inhibition	22.750	22.820	1.003

HLM: Human liver microsomes, RLM: Rat liver microsomes.

Table 3. IC_{50} values and inhibition of dapson metabolism by fisetin in RLM and HLM.

	IC_{50} Value (μM)	Inhibition type	K_i (μM)	αK_i (μM)	α
RLM	4.97	Non-competitive inhibition	6.858	7.957	1.160
HLM	15.00	Mixed inhibition	13.190	32.810	2.487

HLM: Human liver microsomes, RLM: Rat liver microsomes.

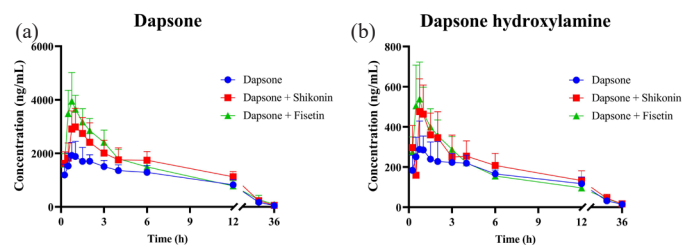


Figure 9. (a) Plasma concentration-time curves of dapson and (b) dapson hydroxylamine after administration alone and in combination. (mean \pm SD, $n = 5$).

to the control group, plasma exposure to dapson was also observed to increase following combined administration of fisetin. The $AUC_{(0-1)}$ and $AUC_{(0-\infty)}$ exhibited a 0.30- and 0.33-fold increase, respectively, while the C_{max} demonstrated a one-fold increase. In contrast, $CL_{z/F}$ was

Table 4. Pharmacokinetic parameters of dapstone in the single administration group and the combined administration group.

Parameters	Dapstone	Dapstone + shikonin	Dapstone + fisetin
AUC _(0-t) (ng/mL ² h)	22454.27 ± 3142.08	30722.37 ± 4102.65**	29297.81 ± 3814.98*
AUC _(0-∞) (ng/mL ² h)	23013.71 ± 3015.26	31250.69 ± 3999.72*	30493.55 ± 5178.92*
t _{1/2} (h)	6.72 ± 1.23	5.91 ± 1.16	7.36 ± 2.17
T _{max} (h)	1.30 ± 0.65	1.15 ± 0.34	0.85 ± 0.14
CL _{z/F} (L/h/kg)	0.44 ± 0.06	0.32 ± 0.04**	0.34 ± 0.06*
C _{max} (ng/mL)	2012.60 ± 523.88	3062.29 ± 636.16	3998.43 ± 1049.56**

* P < 0.05, ** P < 0.01, compared with dapstone group alone. AUC: Area under the plasma concentration-time curve; t_{1/2}: Elimination half-life; T_{max}: Peak time; CL_{z/F}: Plasma clearance; C_{max}: Maximum plasma concentration. (mean ± SD, n = 5).

Table 5. Pharmacokinetic parameters of dapstone hydroxylamine in the single administration group and the combined administration group.

Parameters	Dapstone	Dapstone + shikonin	Dapstone + fisetin
AUC _(0-t) (ng/mL ² h)	3318.93 ± 440.88	4145.44 ± 1024.03	3679.94 ± 612.67
AUC _(0-∞) (ng/mL ² h)	3463.84 ± 440.32	4315.85 ± 1049.65	3908.19 ± 606.05
t _{1/2} (h)	7.97 ± 0.63	7.85 ± 1.22	9.19 ± 2.15
T _{max} (h)	0.75 ± 0.18	0.80 ± 0.11	0.75 ± 0.00
CL _{z/F} (L/h/kg)	2.93 ± 0.38	2.46 ± 0.76	2.61 ± 0.45
C _{max} (ng/mL)	324.57 ± 90.86	500.31 ± 159.33	538.76 ± 184.31

AUC: Area under the plasma concentration-time curve; t_{1/2}: Elimination half-life; T_{max}: Peak time; CL_{z/F}: Plasma clearance; C_{max}: Maximum plasma concentration. (mean ± SD, n = 5).

significantly reduced by 0.23 times (from 0.44 ± 0.06 L/h/kg to 0.34 ± 0.06 L/h/kg). Following the combined administration of shikonin or fisetin, there were no statistically significant changes in the parameters of dapstone hydroxylamine. Nevertheless, its AUC_(0-t) and AUC_(0-∞) exhibited a tendency to increase. The individual pharmacokinetic data for dapstone and dapstone hydroxylamine have been presented in Tables 4 and 5, respectively. In summary, shikonin and fisetin had been shown to inhibit dapstone metabolism *in vivo*.

3.5 Discussion

Dapstone has been granted approval by the United States Food and Drug Administration (FDA) for the treatment of leprosy and dermatitis herpetiformis. Additionally, it has been demonstrated to be an effective preventative measure against pneumocystis pneumonia in patients with HIV disease [21,22]. Due to its antioxidant, anti-inflammatory and anti-apoptotic properties, it is a widely used treatment for various inflammatory and infectious skin diseases [23]. However, treatment with dapstone frequently results in blood toxicity and other adverse effects [24]. Dapstone and its N-hydroxylated metabolite (dapstone hydroxylamine) have demonstrated the capabilities to obstruct bile flow and induce liver necrosis, which can subsequently lead to hemolysis and ultimately hepatitis [25]. Accordingly, when dapstone is administered concurrently with P450 inhibitors or inducers, it is imperative to closely monitor plasma concentrations of dapstone and dapstone hydroxylamine to mitigate the risk of adverse effects.

In vitro studies, we screened out the drugs that were more likely to interact with dapstone from 48 traditional Chinese medicines. A total of 48 traditional Chinese medicines were screened, and 16 were found to have an inhibition rate greater than 80% for dapstone. Two traditional Chinese medicines were selected, which showed potential inhibition of dapstone metabolism. In RLM, the IC₅₀ values of shikonin and fisetin were 12.21 μM and 4.97 μM, respectively. The inhibition types were identified as non-competitive, indicating that the two drugs inhibited dapstone metabolism in a similar manner in RLM. Nevertheless, fisetin exhibited a more pronounced inhibitory effect (with an IC₅₀ value lower than that of shikonin). In HLM, the IC₅₀ values of shikonin and fisetin were 31.39 μM and 15.00 μM, respectively, and the inhibition types were non-competitive inhibition and mixed inhibition, respectively. The findings suggested that the two drugs exhibited disparate inhibition mechanisms with respect to dapstone in HLM. Similarly, fisetin exhibited a more pronounced inhibitory effect, with an IC₅₀ value that was approximately half that of shikonin.

The effects of shikonin and fisetin on the metabolism of dapstone were evaluated using *in vivo* studies. The results demonstrated that the plasma exposure and bioavailability of dapstone were enhanced following combination with shikonin or fisetin. Following the oral administration of 10 mg/kg dapstone to SD rats, the t_{1/2} and T_{max} of dapstone were observed to be 6.72 ± 1.23 hrs and 1.30 ± 0.65 hrs, respectively. These values were close to those presented in reference (t_{1/2}: 6.76 ± 1.95 h, T_{max}: 1.67 ± 1.01 h) [18]. Following the administration of shikonin, the AUC_(0-t) and AUC_(0-∞) for dapstone exhibited a 0.37 and 0.36 times increase, respectively, while the CL_{z/F} exhibited a significant 0.27-fold reduction when compared against the control group. Following the combination of fisetin, the AUC_(0-t) and AUC_(0-∞) of dapstone exhibited a 0.30 and 0.33-fold increase, respectively, and the C_{max} was also increased significantly from 2012.60 ± 523.88 ng/mL to 3998.43 ± 1049.56 ng/mL. The CL_{z/F} was found to be significantly reduced by 0.23 times. There were no statistically significant changes in the parameters of dapstone hydroxylamine. However, both the AUC_(0-t) and AUC_(0-∞) of dapstone hydroxylamine exhibited an increasing trend. Therefore, when dapstone was combined with shikonin or fisetin, there was a potential increase in toxicity. The results indicated that fisetin enhanced the plasma concentration of dapstone to a greater extent, thereby demonstrating that fisetin inhibited the metabolism of dapstone to a more pronounced degree. This finding was consistent with *in vitro* studies.

The potential mechanisms through which shikonin and fisetin enhanced dapstone plasma exposure are possibly associated with their inhibitory effects on P450 enzymes and/or drug transporter proteins. First, dapstone is primarily metabolized by hepatic CYP3A4 and 2E1 enzymes [4,5], and shikonin and fisetin have the potential to inhibit CYP3A4 enzymes [15,16]. The combined effect of these compounds on P450 enzyme activity results in a reduction of dapstone metabolism rate, leading to an increase in the plasma concentration of dapstone, i.e., an increase in exposure. Secondly, P-glycoprotein, an important drug transporter protein [26], may affect the exocytosis of dapstone by affecting the activity of P-glycoprotein, thus increasing its concentration in plasma.

A study reported that when ambrisentan was co-administered with shikonin, there was a notable increase in the C_{max} and AUC_(0-∞) of ambrisentan, where shikonin demonstrated a significant inhibitory effect on the metabolism of ambrisentan [20]. The co-administration of (-)-epigallocatechin gallate (EGCG) with fisetin resulted in an increase in the plasma exposure of EGCG and a prolongation of its t_{1/2} [27]. These findings collectively illustrated the *in vivo* inhibitory potential of shikonin and fisetin, which aligned with these observations.

In summary, the findings of our study indicated that both shikonin and fisetin exerted inhibitory effects on the metabolism of dapstone. However, fisetin exhibited a more pronounced inhibitory effect on dapstone metabolism and a more substantial impact on plasma exposure of dapstone. It is therefore important to monitor the plasma concentrations of dapstone and dapstone hydroxylamine when dapstone is combined with shikonin or fisetin in clinical practice, and to adjust the administered dose in a timely manner to reduce the risk of hematological toxicity.

4. Conclusions

This study successfully screened 16 traditional Chinese medicines with greater than 80% inhibition of dapstone metabolism. Furthermore, the *in vivo* and *in vitro* interactions of shikonin and fisetin with dapstone were thoroughly investigated. It was confirmed that shikonin and fisetin could inhibit the metabolism of dapstone *in vivo* and *in vitro*, with fisetin exhibiting a more pronounced inhibitory effect. Furthermore, this study aimed to provide data for the clinical combination of dapstone with shikonin or fisetin, with the administration dose being adjusted as appropriate to achieve the optimal therapeutic outcome.

CRedit authorship contribution statement

Hualu Wu: Conceptualization, Data curation, Formal analysis, Investigation, Writing – original draft. **Haixin Fu:** Supervision,

Writing – review & editing. **Jun Wu:** Investigation, Methodology, Visualization, Writing – original draft. **Peiqi Wang:** Writing –review & editing. **Yuxin Shen:** Writing – review & editing. **Lu Shi:** Supervision, Conceptualization. **Ren-ai Xu:** Conceptualization.

Declaration of competing interest

The authors declare that they have no known competing financial interests or personal relationships that could have appeared to influence the work reported in this paper.

Declaration of Generative AI and AI-assisted technologies in the writing process

The authors confirm that there was no use of artificial intelligence (AI)-assisted technology for assisting in the writing or editing of the manuscript and no images were manipulated using AI.

References

- Diaz-Ruiz, A., Nader-Kawachi, J., Calderón-Estrella, F., Mata-Bermudez, A., Alvarez-Mejia, L., Ríos, C., 2022. Dapsone, More than an Effective Neuro and Cytoprotective Drug. *Current Neuropharmacology*, **20**, 194-210. <https://doi.org/10.2174/1570159x19666210617143108>
- Wang, Z.Z., Zeng, R., Wu, Z.W., Wang, C., Jiang, H.Q., Wang, H.S., 2023. Overview and Current Advances in Dapsone Hypersensitivity Syndrome. *Current Allergy and Asthma Reports*, **23**, 635-645. <https://doi.org/10.1007/s11882-023-01109-7>
- Coleman, M.D., 1993. Dapsone: modes of action, toxicity and possible strategies for increasing patient tolerance. *The British Journal of Dermatology*, **129**, 507-513. <https://doi.org/10.1111/j.1365-2133.1993.tb00476.x>
- Fleming, C.M., Branch, R.A., Wilkinson, G.R., Guengerich, F.P., 1992. Human liver microsomal N-hydroxylation of dapsone by cytochrome P-4503A4. *Molecular Pharmacology*, **41**, 975-980. <https://molpharm.aspetjournals.org/content/41/5/975.long>
- Mitra, A.K., Thummel, K.E., Kalhorn, T.F., Kharasch, E.D., Unadkat, J.D., Slattery, J.T., 1995. Metabolism of dapsone to its hydroxylamine by CYP2E1 in vitro and in vivo. *Clinical Pharmacology and Therapeutics*, **58**, 556-566. [https://doi.org/10.1016/0009-9236\(95\)90176-0](https://doi.org/10.1016/0009-9236(95)90176-0)
- Bian, Y., Kim, K., An, G.J., Ngo, T., Bae, O.N., Lim, K.M., Chung, J.H., 2019. Dapsone Hydroxylamine, an Active Metabolite of Dapsone, Can Promote the Procoagulant Activity of Red Blood Cells and Thrombosis. *Toxicological Sciences*, **172**, 435-444. <https://doi.org/10.1093/toxsci/kfz188>
- Dziewulska, K.H., Reisz, J.A., Hay, A.M., D'Alessandro, A., Zimring, J.C., 2023. Hemolysis and Metabolic Lesion of G6PD Deficient RBCs in Response to Dapsone Hydroxylamine in a Humanized Mouse Model. *The Journal of Pharmacology and Experimental Therapeutics*, **386**, 323-330. <https://doi.org/10.1124/jpet.123.001634>
- Huang, Y., Cai, T., Xia, X., Cai, Y., Wu, X.Y., 2016. Research Advances in the Intervention of Inflammation and Cancer by Active Ingredients of Traditional Chinese Medicine. *Journal of Pharmacy & Pharmaceutical Sciences*, **19**, 114-126. <https://doi.org/10.18433/j3sg7k>
- Guo, C., He, J., Song, X., Tan, L., Wang, M., Jiang, P., Li, Y., Cao, Z., Peng, C., 2019. Pharmacological properties and derivatives of shikonin-A review in recent years. *Pharmacological Research*, **149**, 104463. <https://doi.org/10.1016/j.phrs.2019.104463>
- Cao, Z., Guo, C., Chen, G., Liu, J., Ni, H., Liu, F., Xiong, G., Liao, X., Lu, H., 2022. Shikonin Inhibits Fin Regeneration in Zebrafish Larvae. *Cells*, **11**, <https://doi.org/10.3390/cells11203187>
- Song, Y., Ding, Q., Hao, Y., Cui, B., Ding, C., Gao, F., 2023. Pharmacological Effects of Shikonin and Its Potential in Skin Repair: A Review. *Molecules*, **28**, 7950. <https://doi.org/10.3390/molecules28247950>
- Ding, H., Li, Y., Chen, S., Wen, Y., Zhang, S., Luo, E., Li, X., Zhong, W., Zeng, H., 2022. Fisetin ameliorates cognitive impairment by activating mitophagy and suppressing neuroinflammation in rats with sepsis-associated encephalopathy. *CNS Neuroscience & Therapeutics*, **28**, 247-258. <https://doi.org/10.1111/cns.13765>
- Hassani, S., Maghsoudi, H., Fattahi, F., Malekinejad, F., Hajmalek, N., Sheikhnia, F., Kheradmand, F., Fahimirad, S., Ghorbanpour, M., 2023. Flavonoids nanostructures promising therapeutic efficiencies in colorectal cancer. *International Journal of Biological Macromolecules*, **241**, 124508. <https://doi.org/10.1016/j.ijbiomac.2023.124508>
- Roy, T., Banang-Mbeumi, S., Boateng, S.T., Ruiz, E.M., Chamcheu, R.N., Kang, L., King, J.A., Walker, A.L., Nagalo, B.M., Kousoulas, K.G., Esnault, S., Huang, S., Chamcheu, J.C., 2022. Dual targeting of mTOR/IL-17A and autophagy by fisetin alleviates psoriasis-like skin inflammation. *Frontiers in Immunology*, **13**, 1075804. <https://doi.org/10.3389/fimmu.2022.1075804>
- Jung, H., Lee, S., 2014. Inhibition of Human Cytochrome P450 Enzymes by Allergen Removed Rhus verniciflua Stoke Standardized Extract and Constituents. *Evidence-based Complementary and Alternative Medic*, **2014**, 150351. <https://doi.org/10.1155/2014/150351>
- Tang, S., Chen, A., Zhou, X., Zeng, L., Liu, M., Wang, X., 2017. Assessment of the inhibition risk of shikonin on cytochrome P450 via cocktail inhibition assay. *Toxicology Letters*, **281**, 74-83. <https://doi.org/10.1016/j.toxlet.2017.09.014>
- Li, Q., Wang, J., Wang, Z.L., Shen, Y., Zhou, Q., Liu, Y.N., Hu, G.X., Cai, J.P., Xu, R.A., 2023. The impacts of CYP3A4 genetic polymorphism and drug interactions on the metabolism of lurasidone. *Biomedicine & Pharmacotherapy*, **168**, 115833. <https://doi.org/10.1016/j.biopha.2023.115833>
- Liu, Y., Li, X., Yang, C., Tai, S., Zhang, X., Liu, G., 2013. UPLC-MS-MS method for simultaneous determination of caffeine, tolbutamide, metoprolol, and dapsone in rat plasma and its application to cytochrome P450 activity study in rats. *Journal of Chromatographic Science*, **51**, 26-32. <https://doi.org/10.1093/chromsci/bms100>
- Kim, J.A., Lee, S., Kim, D.E., Kim, M., Kwon, B.M., Han, D.C., 2015. Fisetin, a dietary flavonoid, induces apoptosis of cancer cells by inhibiting HSF1 activity through blocking its binding to the hsp70 promoter. *Carcinogenesis*, **36**, 696-706. <https://doi.org/10.1093/carcin/bgv045>
- Lan, T., Fang, P., Ye, X., Lan, X., Xu, R.A., 2021. Evaluation of herb-drug interaction of ambrisentan with shikonin based on UPLC-MS/MS. *Le Pharmacien Biologiste*, **59**, 1133-38. <https://doi.org/10.1080/13880209.2021.1964544>
- Paniker, U., Levine, N., 2001. Dapsone and sulfapyridine. *Dermatologic Clinics*, **19**, 79-86, viii. [https://doi.org/10.1016/s0733-8635\(05\)70231-x](https://doi.org/10.1016/s0733-8635(05)70231-x)
- Kurien, G., Jamil, R.T., Preuss, C.V., 2024. Dapsone. StatPearls. Treasure Island (FL) ineligible companies. Disclosure: Radia Jamil declares no relevant financial relationships with ineligible companies. Disclosure: Charles Preuss declares no relevant financial relationships with ineligible companies., StatPearls Publishing Copyright © 2024, StatPearls Publishing LLC.
- Khalilzadeh, M., Shayan, M., Jourian, S., Rahimi, M., Sheibani, M., Dehpour, A.R., 2022. A comprehensive insight into the anti-inflammatory properties of dapsone. *Naunyn Schmiedeberg's Archives of Pharmacology*, **395**, 1509-1523. <https://doi.org/10.1007/s00210-022-02297-1>
- Pickert, A., Raimer, S., 2009. An evaluation of dapsone gel 5% in the treatment of acne vulgaris. *Expert Opinion on Pharmacotherapy*, **10**, 1515-1521. <https://doi.org/10.1517/14656560903002097>
- Ezhilarasan, D., 2021. Dapsone-induced hepatic complications: it's time to think beyond methemoglobinemia. *Drug and Chemical Toxicology*, **44**, 330-33. <https://doi.org/10.1080/01480545.2019.1679829>
- Kanado, Y., Tsurudome, Y., Omata, Y., Yasukochi, S., Kusunose, N., Akamine, T., Matsunaga, N., Koyanagi, S., Ohdo, S., 2019. Estradiol regulation of P-glycoprotein expression in mouse kidney and human tubular epithelial cells, implication for renal clearance of drugs. *Biochemical and Biophysical Research Communication*, **519**, 613-19. <https://doi.org/10.1016/j.bbrc.2019.09.021>
- Chung, J.O., Lee, S.B., Jeong, K.H., Song, J.H., Kim, S.K., Joo, K.M., Jeong, H.W., Choi, J.K., Kim, J.K., Kim, W.G., Shin, S.S., Shim, S.M., 2018. Quercetin and fisetin enhanced the small intestine cellular uptake and plasma levels of epi-catechins in vitro and in vivo models. *Food Functional*, **9**, 234-242. <https://doi.org/10.1039/c7f001576c>